Faculty of Medicine and Life Sciences
School for Life Sciences

Master of Biomedical Sciences

Master's thesis

Influence of the loss of enteric neuronal Ndrg4 on neuronal density and immunological phenotype of the colon

Loriane Verleye

Thesis presented in fulfillment of the requirements for the degree of Master of Biomedical Sciences, specialization Environmental Health Sciences

SUPERVISOR :
Dr. Veerle MELOTTE

MENTOR :
Drs. Meike THIJSSEN

2022
2023

Faculty of Medicine and Life Sciences
School for Life Sciences

Master of Biomedical Sciences

Master's thesis

Influence of the loss of enteric neuronal Ndrg4 on neuronal density and immunological phenotype of the colon

Loriane Verleye
Thesis presented in fulfillment of the requirements for the degree of Master of Biomedical Sciences, specialization Environmental Health Sciences

SUPERVISOR :
Dr. Veerle MELOTTE

MENTOR :
Drs. Meike THIJSSEN

Influence of the loss of enteric neuronal Ndrg4 on neuronal density and immunological phenotype of the colon*

Loriane Verleye[1], Meike Thijssen[1,2], Marion Gijbels[1,3,4], Nathalie Vaes[2], and Veerle Melotte[1,5]

[1]Department of Pathology, GROW-School for Oncology and Reproduction, Maastricht University Medical Centre, 6229 HX Maastricht, The Netherlands
[2]Biomedical Research Institute (BIOMED), Hasselt University, 3950 Diepenbeek, Belgium
[3]Departments of Pathology and Molecular Genetics, Cardiovascular Research Institute Maastricht (CARIM), Maastricht University Medical Centre, 6229 HX Maastricht, The Netherlands
[4]Department of Medical Biochemistry, Academic Medical Center, 1105 AZ Amsterdam, The Netherlands
[5]Department of Clinical Genetics, Erasmus MC University Medical Centre, 3015 GD Rotterdam, The Netherlands

*Running title: *Enteric neuronal Ndrg4 loss on neurons and colon.*

Corresponding author: Veerle Melotte, email: veerle.melotte@maastrichtuniversity.nl

Keywords: neurogastroenterology, enteric nervous system, NDRG4, tumour microenvironment, intestinal inflammation

ABSTRACT

Recently, neurosciences attracted more attention in the field of oncology, also in the context of colorectal cancer (CRC). The colon is highly innervated and even harbours a huge intrinsic nervous system: the enteric nervous system (ENS). Our group has revealed that N-Myc Downstream-Regulated Gene 4 (NDRG4), an early detection biomarker for CRC, is specifically expressed in enteric neurons, and that loss of Ndrg4 protein promotes CRC. Moreover, we observed that Ndrg4^{-/-} mice were more vulnerable to a colitis-induced CRC protocol. The aim of this study was to investigate the impact of the enteric neural loss of Ndrg4 on enteric neuronal density and colon inflammation. To do so, we induced colitis in enteric neural specific Ndrg4 knock-out mice (Ndrg4^{fl/fl}/Wnt1Cre2) using 3% dextran sulphate sodium (DSS). Our results elucidate that there were no differences in enteric neuronal density between Ndrg4^{fl/fl}/Wnt1Cre2 and wild-type mice after staining for pan-neuronal marker Hu in the myenteric plexus. Moreover, no differences in inflammation severity were observed in colon sections of Ndrg4^{fl/fl}/Wnt1Cre2 and wild-type mice which received DSS. Cell profiling of different immune cells, using flow cytometry, revealed a significantly decreased percentage of B cells and neutrophils in colon lamina propria of Ndrg4^{fl/fl}/Wnt1Cre2 mice compared to wild-type mice. In conclusion, our results suggest that Ndrg4 loss in enteric neurons neither influences enteric neuronal density nor colon inflammation. However, immunological phenotype seems to be affected upon Ndrg4 loss.

INTRODUCTION

In 2020, colorectal cancer (CRC) ranked as the third most incident cancer type after breast and lung cancers, with an estimation of about two million new CRC cases worldwide (1). Although advances in screening techniques detecting pre-cancerous polyps and/or early-stage CRC developed over the years, CRC still ranks as the second most lethal cancer type worldwide, with one million deaths caused by CRC (1–3). Several factors can partly explain this high mortality rate. One of the factors influencing the high lethality of CRC is the lack of treatment response and/or limited options for personalised therapy.

While it has been known for years that CRC results because of an accumulation of genetics or epigenetic events, research focuses now also on the tumour microenvironment (TME) (4,5). Different cell types comprise the colorectal TME, including immune cells, neuroendocrine cells and epithelial cells, but also the vasculature irrigating the tumour, the microbiota or extracellular matrix (6–8). More recently, another TME component which could

influence the development and progression of CRC has reached the spotlight: the nervous system (9).

The gastrointestinal (GI) tract is a particularly highly innervated organ; while the sympathetic and parasympathetic nervous systems provide the GI tract with extrinsic innervation (i.e. the neuronal cell bodies lie outside the gut wall), it also benefits from its own innervation, namely the enteric nervous system (ENS) (10,11). The ENS, also called the guts own brain, demonstrates different roles for good functioning of the GI tract, including motility control and regulation of the intestinal permeability (9). Therefore, a defective ENS can lead to neuropathies (e.g. Hirschsprung's disease, achalasia) or inflammatory conditions (e.g. inflammatory bowel disease (IBD)) (12). The influence of an altered ENS on inflammation in the colon was already studied in two mouse models. For example, Margolis *et al.* (2011) induced colitis in mice using dextran sulphate sodium (DSS) in water to induce gut inflammation and has shown that mice with a fewer number of enteric neurons ($Hand2^{+/-}$ mice) showed significantly reduced inflammation severity in the colon compared to their wild-type counterparts (13). On the other hand, mice with more enteric neurons than normal (NSE-noggin mice) suffered from a significantly higher inflammation severity compared to wild-type animals (13).

Recently, our group showed a role of the enteric neuronal specific protein N-Myc Downstream-Regulated Gene 4 (NDRG4) in CRC. NDRG4 DNA promoter methylation is a well-established early detection biomarker for CRC, which is currently enrolled in a FDA-approved multi-target stool DNA screening test (Cologuard®, Exact Sciences Corporation, Madison, USA) screening for CRC (14,15). After demonstrating that Ndrg4 is specifically expressed in enteric neurons, Vaes *et al.* (2021) revealed that loss of Ndrg4 promotes CRC by an increased release of the extracellular matrix proteins Fibulin-2 and Nidogen-1 (5,15).

Interestingly, preliminary data from our group have also shown that $Ndrg4^{-/-}$ mice are more vulnerable to an azoxymethane (AOM)/DSS protocol causing colitis-associated CRC in mice, compared to wild-type mice. This was characterised by an increased percentage of weight loss but also an increased death rate of $NDRG4^{-/-}$ mice (40%) compared to $Ndrg4^{+/+}$ mice (10-15%) (unpublished data).

With the current study, we aim to investigate whether this effect is due to an altered neuronal density upon loss of NDRG4. Moreover, we aim to investigate the impact of NDRG4 loss on colon inflammation and different immune subtypes after an acute DSS treatment.

EXPERIMENTAL PROCEDURES

Mice - $Ndrg4^{fl/fl}$/Wnt1Cre2 mice, where NDRG4 is specifically knocked out in enteric neurons by expression of Cre under the Wnt1 promoter and $Ndrg4^{fl/fl}$ (wild-type) mice were bred. All mice sacrifices were performed using CO_2 asphyxia. All animal experiments were approved by the Committee of Animal Welfare of Maastricht University and performed according to Dutch regulations.

Prior to experiment, all animals were characterised by genotyping PCR. DNA was extracted from toes by incubation in 75µL of 50mM KOH at 95ºC for 1h in the Biorad T100TM thermal cycler (Biorad). PCR was performed using the Biorad T100TM thermal cycler (Biorad) with the conditions mentioned in Figure S1. The PCR reaction mix contained 10µL REDExtract-N-Amp PCR Reaction Mix (REDExtract-N-AmpTM Tissue PCR Kit, Sigma-Aldrich, St. Louis, MO, USA), 0.8µL Wnt1Cre2 primer mix (10µM) as listed in Table S1 and 2µL of sample diluted at 1:50 in sterile H_2O, in a final volume of 20µL. PCR product was detected in a 1.5% (w/v) agarose gel in 0.5x Tris-borate-EDTA (TBE) buffer at 130V for 25 minutes

Neuronal density in the colon - Three $Ndrg4^{fl/fl}$ wild-type and five $Ndrg4^{fl/fl}$/Wnt1Cre2 hemizygous mice were age-, nest- and gender-matched and socially housed in ventilated cages with water and food *ad libitum*. All mice were sacrificed between the age of eight to twelve weeks.

Tissue preparation - After sacrifice, the abdomen was opened and the GI tract (i.e. from the stomach to the anus) was harvested and stored in phosphate-buffered saline (PBS) solution on ice until further processing. First, the colon was cut from the caecum and cleaned from fat and other residues. Colon length was measured before the organ was cut open with scissors for stool removal.

	DAY 1	DAY 2	DAY 3	DAY 4	DAY 5	DAY 6	DAY 7	DAY 8	DAY 9
MORNING									
AFTERNOON									

Figure 1. Timeline representing the administration of fresh water containing 3% DSS (grey), fresh water (blue) and sacrifice for the different experiments involving the induction of acute inflammation.

Afterwards, the colon tissue was transferred onto a Sylgard-coated Petri dish (Sylgard 184 Elastomer, Down Corning, Auburn, MI, USA) with PBS where the colon was pinned flat using insect pins (0.2 mm, Agar Scientific, Stansted, UK), with the mucosa side up. The mucosal layer and the submucosal plexus were removed from the underlying muscle and myenteric plexus layers using forceps. After fixation in 4% paraformaldehyde (PFA) for 45 minutes, the tissue was rinsed three times for a total of 45 minutes in PBS. Finally, the colon was cut in approximately equal parts of 15mm and stored in 0.01% sodium azide-PBS solution at 4ºC.

Immunofluorescence staining - For each colon, the most distal piece of tissue was selected for immunofluorescence staining. Fixated tissues were blocked with 4% donkey serum in 1% Triton X-100 in PBS (i.e. blocking medium) for two hours at room temperature (RT) to allow permeabilisation and blocking of non-specific binding. Afterwards, tissues were incubated at 4ºC overnight with the primary antibody human Hu (gift from Vanda Lennon) diluted at 1:10,000 in the blocking medium. After overnight incubation, tissues were washed three times for ten minutes in PBS before an incubation of two hours in the dark at 4ºC with the secondary antibody goat anti-human Alexa 594 diluted at 1:1,000 (A-11014, Thermofisher). After PBS washing, tissue sections were mounted on glass slides with CitiFluor^{TM} AF1, Mounting Medium (E17970-25, EMS) and covered with coverslide.

Imaging and cell counting - A Leica M165 FC microscope (Leica Microsystems) was used to picture at least two non-overlapping tile scans of each stained tissue. Hu+ cells were manually counted using the Cell Counter plugin in ImageJ2 version 2.9.0/1.53t (NIH, Bethesda, MD). The cell number per region was averaged per mouse and was normalised for colon stretching by multiplying this averaged number by a factor calculated as the total stretched colon length after dissection divided by the total colon length before dissection.

Induction of acute intestinal inflammation -
Acute intestinal inflammation was induced using three cycles of 3% DSS in sterilised tap water. Figure 1 shows the timeline to induce acute inflammation and sacrifice for each experiment.

Visual characterisation of acute intestinal inflammation - Seven Ndrg4^{fl/fl} wild-type and six Ndrg4^{fl/fl}/Wnt1Cre2 mice were sacrificed after DSS treatment at the age of 14 weeks. After sacrifice, the small intestine, colon and spleen were harvested. Mesentery was removed from the small intestine and the colon before the tissues were cut open and cleaned from stool. The small intestine was cut into three approximately equal parts to form the duodenum, jejunum and ileum. As previously described, these three parts and the colon were rolled like a "Swiss roll", starting from the proximal part to the distal part (16). Afterwards, tissues were fixed in a cassette in 4% PFA for 24 hours and washed with PBS. Thereafter, Swiss rolls and spleen were immersed in 15% sucrose-PBS solution for four hours before being immersed into 30% sucrose-PBS solution overnight. The day after, Swiss rolls and spleens were cut in half before embedding in TissueTek® (4583, Sakura). Directly after, the organ blocks were frozen on dry ice in a dish with isopentane and kept at -80ºC until processing.

Staining - For each mouse, a 5µm section cut using a Leica CM3050 S cryostat (Leica Biosystems) was stained with haematoxylin and eosin according to standard procedure.

Visual characterisation - The presence of inflammation and specific immune cells was visually characterised by an experienced animal

pathologist (M.G.). Inflammation severity was assessed by comparing inflammation across samples and by giving a score between 0 (no inflammation) and 4 (most severe inflammation). For each sample, the percentage of plasma cells and granulocytes across the section was also estimated. Images were acquired using a Leica M300 LED microscope with a Leica DFC320 camera (Leica Microsystems) and the QWIN V3 software (Leica).

Flow cytometry analysis - For each experiment, eight Ndrg4$^{fl/fl}$ and eight Ndrg4$^{fl/fl}$Wnt1Cre2 mice were sacrificed at the age of 14 weeks after receiving a DSS treatment. The complete lists of antibodies and solutions used in these experiments are found in Table S2 and Table S3, respectively.

Cell isolation - As previously described, cells were isolated from the colon for the major immune cell populations, and both the colon and mesenteric lymph nodes (MLN) for the analysis B cell subtypes [17]. MLN were stored in cRPMI solution on ice until further processing. Cleaned colon tissues were weighted and cut in one-centimetre pieces. To remove mucus, colon tissues were washed in solution 1 with 1:200 5mM DTT at a volume of 20mL/g pre-warmed shaking at 200RPM for a duration of 15min at 37ºC. To remove epithelial cells, colon tissues were subsequently washed three times in 15mL/g of pre-warmed solution 2 containing 5mM EDTA for 10 min, shaking at 200RPM at 37ºC. Each time, supernatant was passed through a 70µm filter into a tube on ice. Supernatant containing colonic intraepithelial leukocytes (CIEL) was then centrifuged at 300xg for 5min at 4ºC before being washed twice in 5mL cold HBSS + 2% foetal calf serum (FCS). Afterwards, CIEL samples were resuspended in 5mL cRPMI and stored on ice until further processing. Samples with colon lamina propria (CLP) were washed in 5mL solution 3 without Liberase TM shaken at 200RPM for 10min at 37ºC, before discarding supernatant. To induce digestion, CLP samples were minced into fine pieces before incubating in solution 3 with Liberase TM (1:20) at 7mL/g, at 200RPM for 30min at 37ºC. MLN samples were digested by injecting them with 1mL solution 3 with Liberase TM (1:20) and incubated for 30min at 37ºC. Digested tissues were passed three times through an 18G needle and then a 70µm filter into a 50mL tube. Thereafter, 0.5 volume

cRPMI was added to each filter before centrifugation at 300xg for 5min at 4ºC. Afterwards, CLP and MLN samples were washed twice in 5mL HBSS + 2% FCS and centrifuged at 300xg for 5min at 4ºC. CLP, CIEL and MLN samples were resuspended in FACS buffer and transferred to a V-shaped 96-well plate before processing to the staining protocol.

Staining isolated cells - For this protocol, centrifuge was set at 1600rpm for 3min at 4ºC unless mentioned otherwise. After centrifuging the plate containing the samples, samples were washed in 100µL PBS and centrifuged again. To detect living cells, samples were resuspended in 50µL of FcBlock/Life-Dead mix (1:1000 AquaDead and 1:100 Fc receptor block in 50µL PBS), with only PBS for the negative control. After incubating in the dark for 20min on ice, samples were centrifuged and supernatant was removed. Cells were then resuspended in 50µL cell membrane antibodies (Table S2) in FACS buffer and incubated in the dark for 30min on ice. Only FACS buffer was added to the negative control. Afterwards, samples were washed with 150µL FACS buffer and centrifuged. Cells were fixated in 200µL 1% PFA in PBS and incubated in the dark for 15min on ice. Subsequently, samples were resuspended in 100µL FACS buffer and pipetted in FACS tubes.

For intracellular staining, fixation in 1% PFA was replaced by the subsequent steps. First, 200µL freshly prepared fixation/permeabilisation working solution was added to each well. After incubating in the dark for 30min at 4ºC, the plate was centrifuged for 5min and supernatant was removed. Afterwards, samples were washed with 150µL permeabilisation buffer (00-5523-00, eBioscience) twice. Samples were incubated in 40µL intracellular antibody (1:40 FoxP3, Invitrogen, 12-5773-82) in permeabilisation buffer in the dark for 30min at 4ºC. Afterwards, cells were washed first in 150µL permeabilisation buffer and then in 150µL FACS buffer. Finally, samples were resuspended in 100µL of FACS buffer and transferred in FACS tubes.

*Data acquisition* - Data were acquired on the FACS Cytek Aurora using the SpectroFlo® software.

Data analysis - Data were analysed with unpaired t-test for the comparison between Ndrg4$^{fl/fl}$/Wnt1Cre2 and Ndrg4$^{fl/fl}$ mice using Prism 9 for macOS (version 9.5.1 (528), GraphPad. P-value was considered significant at 0.05.

RESULTS

No difference in enteric neuronal density between Ndrg4$^{fl/fl}$Wnt1Cre2 and wild-type mice - Enteric neurons were stained with the pan-neuronal marker Hu in the colon myenteric plexus to visualise enteric neurons (Figure 2A). Statistical analysis performed after cell counting revealed no statistically significant difference in the mean number of neurons per mm^2 (p-value = 0.737). As depicted in Figure 2B, the average number of enteric neurons per mm^2 in Ndrg4$^{fl/fl}$ mice varies between 134 and 172, with a mean of 143 enteric neurons. In Ndrg4$^{fl/fl}$Wnt1Cre2 mice, the mean value varies between 118 and 172, with a mean of 149 enteric neurons per mm^2 of myenteric plexus.

Intestinal inflammation visually characterised as less severe in Ndrg4$^{fl/fl}$Wnt1Cre2 mice - In general, inflammation was observed after acute DSS treatment in both Ndrg4$^{fl/fl}$Wnt1Cre2 and wild-type mice by H&E staining (Figure 3A).
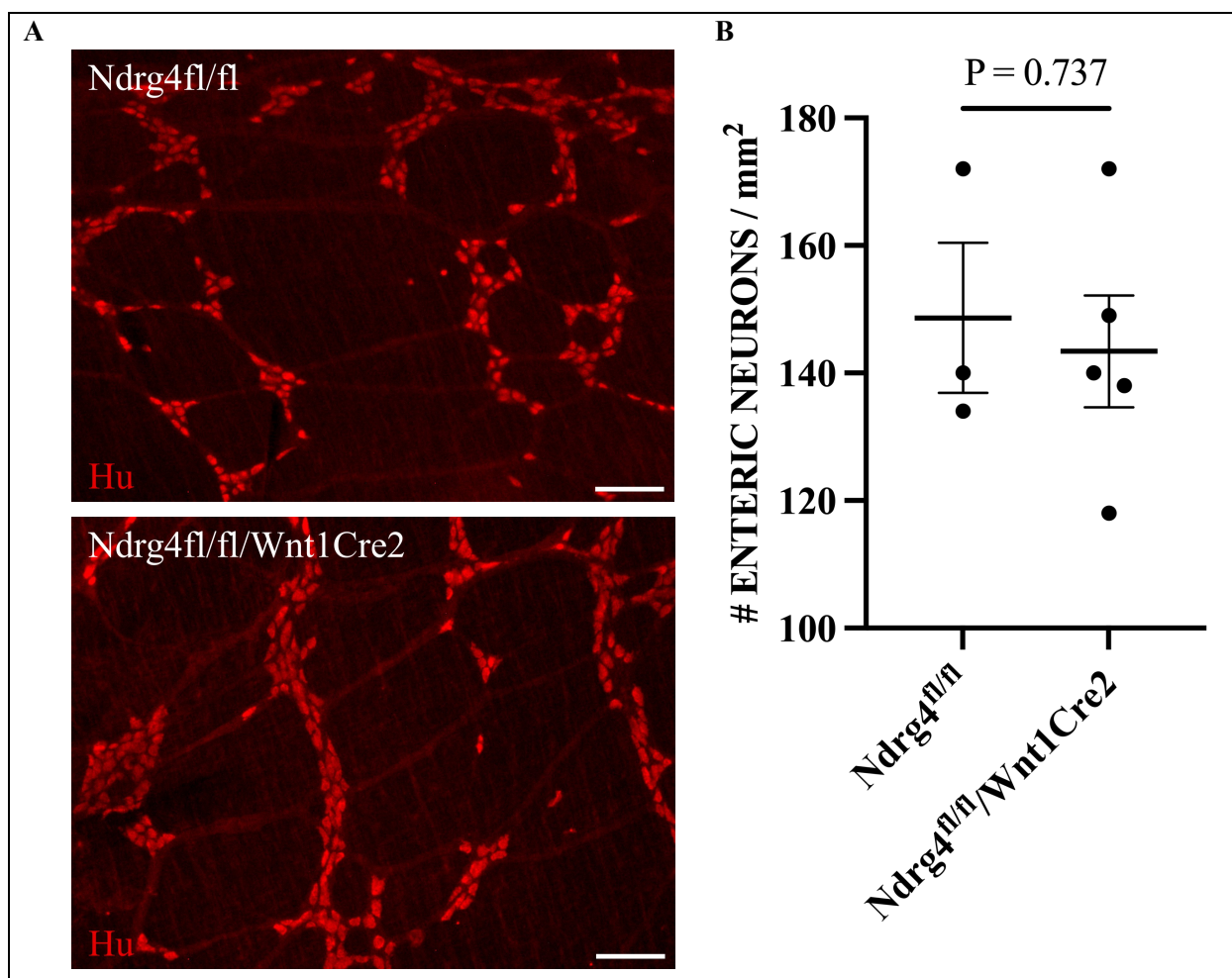
Figure 2. Comparison of the enteric neuronal density between Ndrg4$^{fl/fl}$Wnt1Cre2 and wild-type mice. **A**. Microscopic images of the myenteric plexus stained with the pan-neuronal marker Hu in Ndrg4$^{fl/fl}$ mouse and Ndrg4$^{fl/fl}$/Wnt1Cre2 mouse used for cell counting. **B**. Summary of the average number of enteric neurons counted in the myenteric plexus in the distal colon of Ndrg4$^{fl/fl}$ (N = 3) and Ndrg4$^{fl/fl}$/Wnt1Cre2 (N = 5) mice after correction for colon stretching. Ndrg4$^{fl/fl}$: 143 ± 12; Ndrg4$^{fl/fl}$Wnt1Cre2: 149 ± 8.8. Unpaired t-test with mean ± SEM. Scale bar set at 200μm.
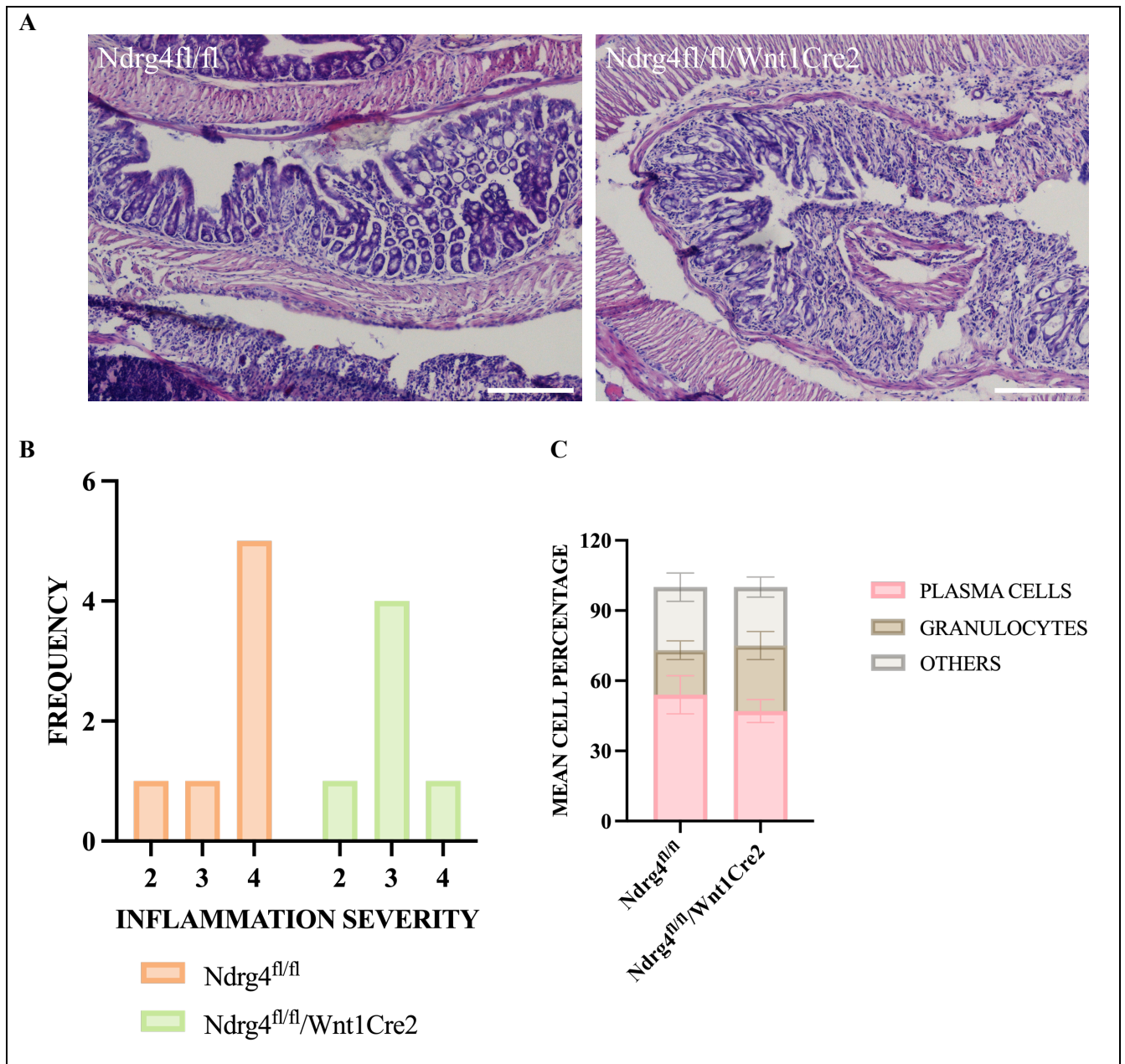
Figure 3. Visual characterisation of acute inflammation. **A**. Microscopic images of colon Swiss rolls after H&E staining in Ndrg4$^{fl/fl}$ (left) and Ndrg4$^{fl/fl}$/Wnt1Cre2 (right) mice treated for eight days with 3% DSS in drinking water, showing inflammation infiltration and immune cells linked with inflammation. **B**. Graphical representation of the frequency each inflammation severity level was chosen after the visual characterization of the Swiss rolls. Most Ndrg4$^{fl/fl}$ (5/7) sections were given a 4 and while the majority of Ndrg4$^{fl/fl}$/Wnt1Cre2 (4/6) sections were given a 3. **C**. Summary of the estimated percentage of certain inflammatory immune cells present in the colon sections analysed. While a higher percentage of granulocytes was observed in colon sections from Ndrg4$^{fl/fl}$/Wnt1Cre2 (25.00% vs 21.67%), the percentage of plasma cells was smaller compared to wild-type mice (46.67% vs 54.29%). However, results were not statistically significant. Unpaired t-test with mean ± SEM. Scale bar set at 200µm.

Inflammation severity was categorically scored between 0 and 4, with 0 indicating no inflammation while 4 indicated extreme inflammation compared to the other tissues. The majority (71%) of tissues from wild-type mice showed the most extreme inflammation level (n°4), while most Ndrg4$^{fl/fl}$Wnt1Cre2 sections (67%) were

depicting severe inflammation (n°3, Figure 3B). No significant differences plasma cells were observed (7.6% ± SEM = 9.9%; p-value = 0.459) between both groups (Figure 3C). However, a higher mean percentage of plasma cells was observed in sections from Ndrg4$^{fl/fl}$ mice (mean = 54.29%; SEM = 8.1%) compared to sections from Ndrg4$^{fl/fl}$Wnt1Cre2 mice
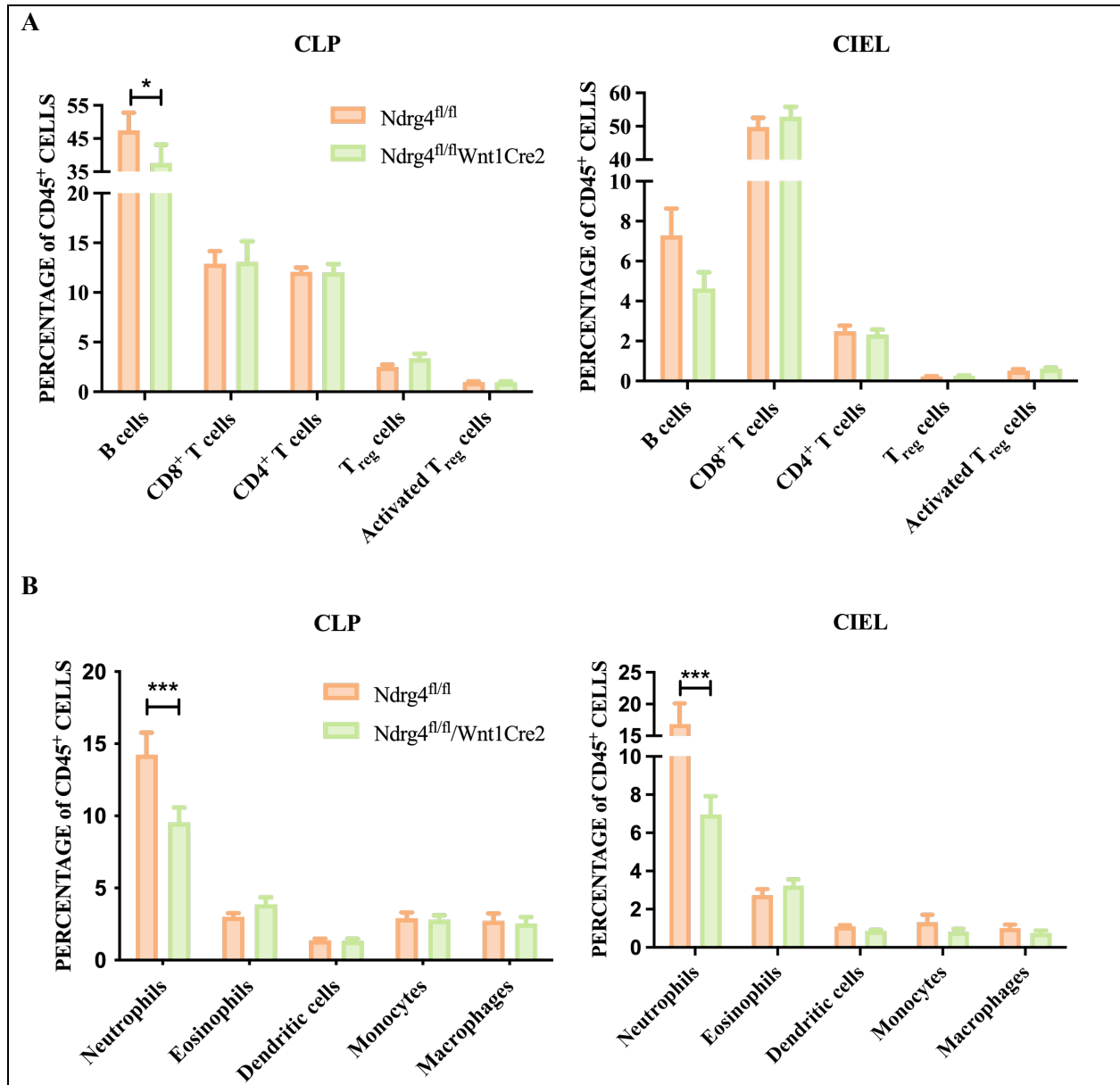
Figure 4. Graphical representation of the major immune cell profiling results. **A**. Results of the analysis of the lymphoid panel showing a decreased B cell percentage in Ndrg4$^{fl/fl}$Wnt1Cre2 mice (N = 8) compared to the wild-type mice (N = 8), which is only significant in the CLP samples (p-value < 0.05). **B**. Results of the analysis of the myeloid panel showing a decreased neutrophils percentage in Ndrg4$^{fl/fl}$Wnt1Cre2 mice compared to the wild-type mice, significant in both CLP and CIEL samples (p-value < 0.001). Bars representing mean and SEM calculated with unpaired t-test.
*Abbreviations* - colon lamina propria (CLP); colonic intraepithelial leukocytes (CIEL)

(mean = 46.67%; SEM = 4.9%). Regarding granulocytes, the mean percentage was higher in colon sections from Ndrg4$^{fl/fl}$Wnt1Cre2 mice (mean = 25.00%; SEM = 4.28%) compared to sections from Ndrg4$^{fl/fl}$ mice (mean = 21.67%; SEM = 3.07%), although the difference was not statistically significant (-3.3 ± 5.3; p-value = 0.541).

In summary, no significant differences in inflammation severity in the colon were observed between Ndrg4$^{fl/fl}$Wnt1Cre2 and wild-type mice.

B cells and neutrophils reduction in colon lamina propria of Ndrg4$^{fl/fl}$Wnt1Cre2 mice - Flow cytometric analysis was performed on the major immune cell populations, including B cells, T cells, neutrophils, eosinophils, dendritic cells, monocytes and macrophages (Table S2). Gating strategies are presented in Figure S2. Statistical analysis revealed statistically significant decreased percentage of B cells analysed in CLP (p-value < 0.05) and of neutrophils in both CLP and CIEL (p-value < 0.001) in Ndrg4$^{fl/fl}$/Wnt1Cre2 compared to wild-type mice. No other significant difference in the other immune cell populations were observed (Figure 4).

No difference in B cell subtypes in the colon and mesenteric lymph nodes between Ndrg4$^{fl/fl}$Wnt1Cre2 and wild-type mice - Based on the results of the immune cell profiling, a second analysis focusing on B cell subtypes was carried out. Figure S3 depicts the gating strategy, including germinal centre B cells, B1b, B1a, memory B cells, IFN-induced B cells and IgM/IgD B cells. Statistical analysis did not reveal statistically significant differences in the percentage each B cell subtype compared to the total number of B cells in CLP and CIEL between Ndrg4$^{fl/fl}$/Wnt1Cre2 and wild-type mice. Analysis of B cell subtypes was also performed in MLN, as these lymph nodes are connected to the colon and they can be seen as a hub for immune cells going to the colon (18). As seen in CLP and CIEL, statistical analysis did not reveal any difference in B cell subtypes between Ndrg4$^{fl/fl}$/Wnt1Cre2 and wild-type mice. Figure 5 depicts the results of the B cell subtypes analysis for CLP and MLN. Results of the analysis in CIEL samples are presented in Figure S4.
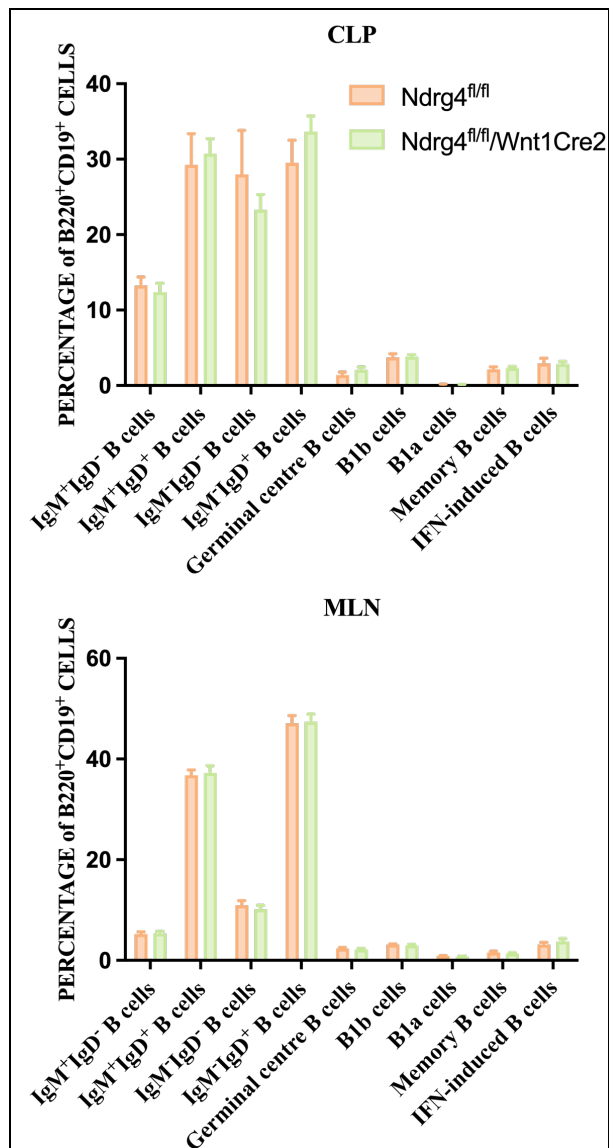
Figure 5. Graphical representation of the B cell subtypes profiling results. No differences in the percentage of different B cell subtypes were observed between Ndrg4$^{fl/fl}$/Wnt1Cre2 (N = 8) and Ndrg4$^{fl/fl}$ mice (N = 8), neither in the CLP samples nor in the MLN samples. Bars representing mean and SEM calculated with unpaired t-test.
Abbreviations - colon lamina propria (CLP); mesenteric lymph nodes (MLN)

DISCUSSION

To our knowledge, we are the firsts to examine the influence of an absence of Ndrg4 in enteric neurons on enteric neuronal density and gut inflammation. NDRG4 has been recognised as an important DNA methylation-based biomarker in the context of CRC which is specifically expressed in enteric neurons (14,15). Preliminary data showed that upon NDRG4 loss, mice were more vulnerable to a colitis-induced CRC treatment, compared to wild-type mice. As it is known that enteric neuronal density can impact gut inflammation (13),we first compared the neuronal density in the colon myenteric plexus of wild-type mice and mice in which Ndrg4 was deleted from enteric neurons (Ndrg4$^{fl/fl}$/Wnt1Cre2). Our findings indicate no statistically significant difference in the neuronal density between Ndrg4$^{fl/fl}$ and Ndrg4$^{fl/fl}$/Wnt1Cre2.

Afterwards, we examined the influence of acute inflammation using the well-established DSS model in both wild-type and Ndrg4$^{fl/fl}$/Wnt1Cre2 mice (19). Although the results were not statistically significant, a lower inflammation severity was suggested in colon sections of Ndrg4$^{fl/fl}$/Wnt1Cre2 mice compared to wild-type mice. Moreover, there was no significant difference in the percentage of plasma cells and granulocytes in the colon sections between Ndrg4$^{fl/fl}$/Wnt1Cre2 and wild-type mice, even though a higher mean percentage of plasma cells and a lower percentage of granulocytes was seen in wild-type mice.

Furthermore, in this study the percentage of the major immune cell population in the different colon layers (CLP and CIEL) was analysed with flow cytometry. It is already known that DSS-induced acute inflammation depends on innate immunity, which comprises different cell types such as macrophages, neutrophils, eosinophils, T cells and dendritic cells, among others (13,20,21). Moreover, it is acknowledged that a bidirectional communication between the ENS and the gastrointestinal immune system exists, with the existence of ENS-immune interactions which functionally modulate intestinal inflammation (12,22). However, the study of the connection between B cells and other immune cells, acute inflammation and the ENS in the context of NDRG4 is so understudied that the current literature does not allow to truly compare our results with other publications. Moreover, the current results also revealed a statistically significant decreased percentage in neutrophils in the CLP and CIEL of Ndrg4$^{fl/fl}$/Wnt1Cre2 mice. This decreased number of neutrophils in Ndrg4$^{fl/fl}$/Wnt1Cre2 mice, who showed less severe inflammation in general, is in line with the role of neutrophils in innate immunity: acting as "first responders" in case of acute inflammation or any other pathogen invasion (23).

B cells are mature haematopoietic stem cells expressing a specific antigen-binding receptor on their membrane, specialised in adaptive immunity (20). We investigated the influence of Ndrg4 absence in the enteric neurons on B cell subtypes. The results demonstrated no statistically significant mean difference in the percentage of the different B cell subtypes for the CLP, CIEL and MLN. However, it is important to note that the B cell subtypes were quantified as fraction of the total B cell population, not the total amount of cells or total amount of immune cells. This means that the absolute number of individual B cell subtypes in the colon can still be changed, however the abundance in the total B cell population is not altered by neuronal density.

Although the present study is innovative as it aims to further understand an understudied topic, it suffers from several limitations. First, enteric neuronal density in the myenteric plexus was only assessed in the distal colon. However, it is known that the enteric nervous system is not heterogeneous throughout the colon (24). For the visual characterisation of acute inflammation, most analysed tissues showed, independently of the mouse genotype, severe to extreme inflammation. Therefore, it may be possible that the DSS treatment was too harsh. Moreover, some pieces of colon were missing in certain sections or the Swiss rolls were not fully formed, which could bias the results. Lastly, the percentage of plasma cells and granulocytes was not a precise percentage. To overcome this limitation, flow cytometry analysis was performed. Another limitation or remark is the DSS protocol to induce acute inflammation in the colon. The percentage of DSS given in the water as well as the number of days for the protocol vary across studies using this method (19,25). Therefore, comparing the effects of a certain genotype on inflammation severity more difficult across studies. However, it could be relevant to test whether different percentages of DSS across different time periods influence inflammation severity in a

specific mouse model. Although this is not a limitation, NDRG4 is mostly studied in the framework of CRC but the current study focused mainly on the possible link between NDRG4, inflammation and the ENS. This study is therefore one step in the understanding of the NDRG4 mechanisms influencing CRC progression through inflammation.

CONCLUSION

In summary, the results of the current study suggest that the absence of Ndrg4 in enteric neurons using the Ndrg4$^{fl/fl}$/Wnt1Cre2 mouse model does not influence the enteric neuronal density in the distal part of the colon. Visual characterisation of acute inflammation in the whole colon revealed a high inflammation severity in both Ndrg4$^{fl/fl}$/Wnt1Cre2 and wild-type mice. Lower neutrophil and B cell percentages were detected in Ndrg4$^{fl/fl}$/Wnt1Cre2 mice compared to their wild-type counterparts. However, no significant differences were observed between wild-type and Ndrg4$^{fl/fl}$/Wnt1Cre2 mice regarding B cell subtypes. In light of these results but also the limitations of the current study, more research is needed to understand further the role of Ndrg4 and the ENS in colonic inflammation and in the end CRC progression.

Maastricht, the Netherlands
Thursday the 8th of June, 2023

REFERENCES

1. Sung H, Ferlay J, Siegel RL, Laversanne M, Soerjomataram I, Jemal A, et al. Global Cancer Statistics 2020: GLOBOCAN Estimates of Incidence and Mortality Worldwide for 36 Cancers in 185 Countries. CA Cancer J Clin. 2021 May;71(3):209–49.

2. Torre LA, Siegel RL, Ward EM, Jemal A. Global cancer incidence and mortality rates and trends - An update. Vol. 25, Cancer Epidemiology Biomarkers and Prevention. American Association for Cancer Research Inc.; 2016. p. 16–27.

3. Issa IA, Nouredine M. Colorectal cancer screening: An updated review of the available options. World J Gastroenterol. 2017 Jul 28;23(28):5086–96.

4. Chen F, Zhuang X, Lin L, Yu P, Wang Y, Shi Y, et al. New horizons in tumor microenvironment biology: Challenges and opportunities. BMC Med. 2015;13(1).

5. Vaes N, Schonkeren SL, Rademakers G, Holland AM, Koch A, Gijbels MJ, et al. Loss of enteric neuronal Ndrg4 promotes colorectal cancer via increased release of Nid1 and Fbln2 . EMBO Rep. 2021;22(6):1–17.

6. Schonkeren SL, Thijssen MS, Vaes N, Boesmans W, Melotte V. The emerging role of nerves and glia in colorectal cancer. Cancers (Basel). 2021;13(1):1–13.

7. Anderson NM, Simon MC. The tumor microenvironment. Curr Biol [Internet]. 2020;30(16):R921–5. Available from: http://dx.doi.org/10.1016/j.cub.2020.06.081

8. Li J, Chen D, Shen M. Tumor Microenvironment Shapes Colorectal Cancer Progression, Metastasis, and Treatment Responses. Front Med. 2022;9(March):1–13.

9. Rademakers G, Vaes N, Schonkeren S, Koch A, Sharkey KA, Melotte V. The role of enteric neurons in the development and progression of colorectal cancer. Biochim Biophys Acta - Rev Cancer. 2017;1868(2):420–34.

10. Furness JB. The enteric nervous system and neurogastroenterology. Nat Rev Gastroenterol Hepatol. 2012;9(5):286–94.

11. Vaes N, Idris M, Boesmans W, Alves M, Melotte V. Nerves in gastrointestinal cancer: from mechanism to modulation. Nat Rev Gastroenterol Hepatol. 2022;

12. Holland AM, Bon-Frauches AC, Keszthelyi D, Melotte V, Boesmans W. The enteric nervous system in gastrointestinal disease etiology. Cell Mol Life Sci [Internet]. 2021;78(10):4713–33. Available from: https://doi.org/10.1007/s00018-021-03812-y

13. Margolis KG, Stevanovic K, Karamooz N, Li ZS, Ahuja A, D'Autréaux F, et al. Enteric neuronal density contributes to the severity of intestinal inflammation. Gastroenterology. 2011;141(2):588–98.

14. Melotte V, Lentjes MHFM, Van Den Bosch SM, Hellebrekers DMEI, De Hoon JPJ, Wouters KAD, et al. N-Myc Downstream-Regulated Gene 4 (NDRG4): A Candidate Tumor Suppressor Gene and Potential Biomarker for Colorectal Cancer. J Natl Cancer Inst. 2009;101(13):916–27.

15. Vaes N, Lentjes MHFM, Gijbels MJ, Rademakers G, Daenen KL, Boesmans W, et al. NDRG4, an early detection marker for colorectal cancer, is specifically expressed in enteric neurons. Neurogastroenterol Motil. 2017;29(9):1–10.

16. Moolenbeek C, Ruitenberg EJ. The "Swiss roll": A simple technique for histological studies of the rodent intestine. Lab Anim. 1981;15(1):57–9.

17. Goodyear AW, Kumar A, Dow S, Ryan EP. Optimization of murine small intestine leukocyte isolation for global immune phenotype analysis. J Immunol Methods [Internet]. 2014;405:97–108. Available from: http://dx.doi.org/10.1016/j.jim.2014.01.014

18. Li H, Fan C, Feng C, Wu Y, Lu H, He P, et al. Inhibition of phosphodiesterase-4 attenuates murine ulcerative colitis through interference with mucosal immunity. Br J Pharmacol. 2019;176(13):2209–26.

19. Chassaing B, Aitken JD, Malleshappa M, Vijay-Kumar M. Dextran sulfate sodium (DSS)-induced colitis in mice. Curr Protoc Immunol. 2014;(SUPPL.104):1–14.

20. Marshall JS, Warrington R, Watson W, Kim HL. An introduction to immunology and immunopathology. Allergy, Asthma Clin Immunol [Internet]. 2018;14(s2):1–10. Available from:

https://doi.org/10.1186/s13223-018-0278-1

21. Melcher C, Yu J, Duong VHH, Westphal K, Helmi Siasi Farimany N, Shaverskyi A, et al. B cell-mediated regulatory mechanisms control tumor-promoting intestinal inflammation. Cell Rep [Internet]. 2022 Jul;40(2):111051. Available from: https://linkinghub.elsevier.com/retrieve/pii/S2211124722008452

22. Wang H, Foong JPP, Harris NL, Bornstein JC. Enteric neuroimmune interactions coordinate intestinal responses in health and disease. Mucosal Immunol. 2022;15(1):27–39.

23. Liew PX, Kubes P. The Neutrophil's Role During Health and Disease. Physiol Rev [Internet]. 2019 Apr 1;99(2):1223–48. Available from: https://www.physiology.org/doi/10.1152/physrev.00012.2018

24. Missiaglia E, Jacobs B, D'Ario G, Di Narzo AF, Soneson C, Budinska E, et al. Distal and proximal colon cancers differ in terms of molecular, pathological, and clinical features. Ann Oncol Off J Eur Soc Med Oncol [Internet]. 2014 Oct;25(10):1995–2001. Available from: https://doi.org/10.1093/annonc/mdu275

25. Kiesler P, Fuss IJ, Strober W. Experimental Models of Inflammatory Bowel Diseases. Cell Mol Gastroenterol Hepatol [Internet]. 2015 Mar 1;1(2):154–70. Available from: http://www.ncbi.nlm.nih.gov/pubmed/26000334

SUPPLEMENTARY MATERIALS

Table S1. Primers and their sequences used for PCR genotyping

target	forward	reverse	product (bp)
Wnt1	CAGCGCCGCAACTATAAGAG		200
Wnt1		CATCGACCGGTAATGCAG	200
Wnt1Cre2	CAGCGCCGCAACTATAAGAG		350
Wnt1Cre2		CATCGACCGGTAATGCAG	350
Abbreviation - base pair (bp)			
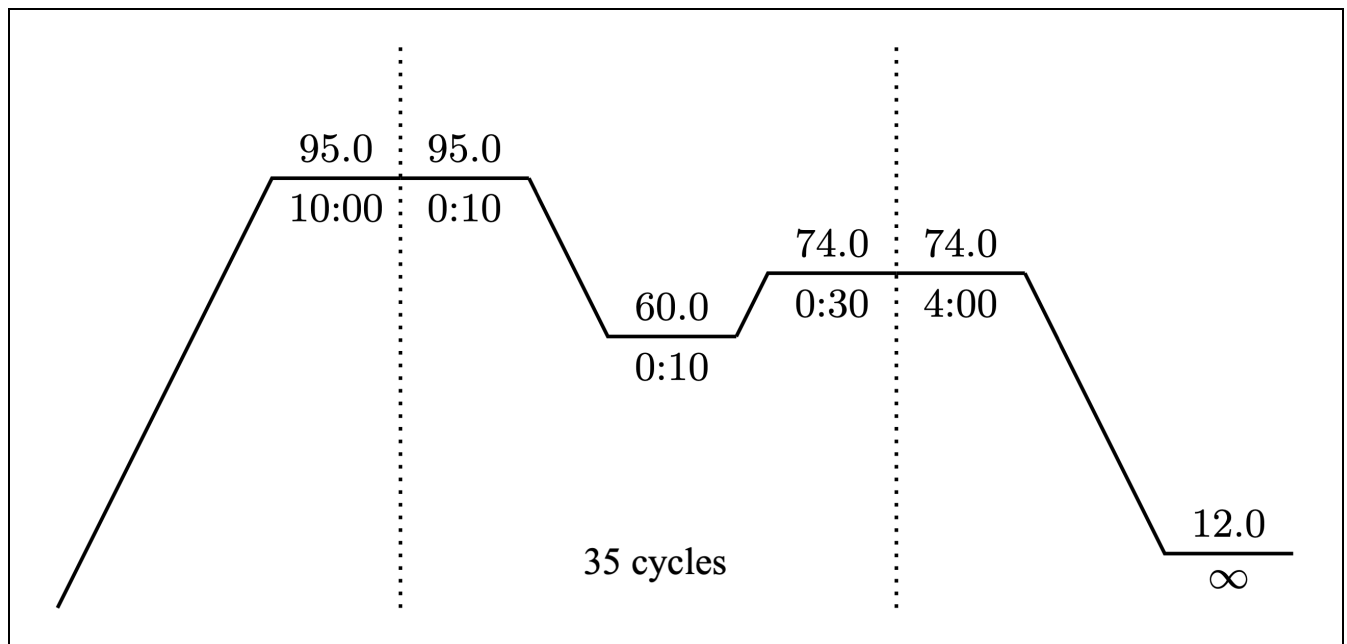
Figure S1. Graphical representation of the PCR program to perform genotyping; 1. initial incubation; 2. annealing; 3. final elongation; temperatures expressed in degree Celsius; time expressed in minutes:seconds.

Table S2. Antibodies used for major immune cell profiling

antigen	fluorochrome	CAB	dilution	supplier	cat. no.
Life/Dead	V500 Aqua	/	1:1000	Invitrogen	10321873
FcBlock	/	360	1:100	Invitrogen	14-0161-85
Major immune cell profiling					
CD45	PerCp	631	1:100	Biolegend	103130
CD3	V450	555	1:100	Invitrogen	48-0032-82
CD4	APC-H7	423	1:100	BD	560181
CD8	FITC	449	1:50	Invitrogen	11-0081-85
CD45R (B220)	SB702	1058	1:100	Invitrogen	67-0452-82
CD25	APC	533	1:100	Invitrogen	17-0251-81
FoxP3	PE	348	1:40	Invitrogen	12-5773-82
MHCII	FITC	451	1:100	Invitrogen	11-5322-82
LY6C	APC	442	1:100	Miltenyi	130-123-769
LY6G	APC-Cy7	612	1:100	BD	560600
F4/80	BV421	806	1:100	Biolegend	123137
CD170 (Siglec-F)	PE	793	1:300	Invitrogen	12-1702-80
CD64	PerCP-eF710	1106	1:100	Invitrogen	46-0641-80
CD11c	PE-Cy7	535	1:100	Invitrogen	25-0114-82
CD11b	EFluor450	616	1:300	Invitrogen	48-0112-80
B cell subtype panel					
CD45	PerCp	631	1:100	Biolegend	103130
CD45R (B220)	SB702	1058	1:100	Invitrogen	67-0452-82
CD3	BUV496		1:50	BD	612955
CD19	BV421	727	1:100	Biolegend	115549
IgA	PE		1:50	Invitrogen	12-4204-81
IgM	APC	775	1:100	BD	550676
IgD	eFluor450	777	1:200	eBioscience	48-5993-82
GL7	PECY7		1:50	Biolegend	144619
CD95	PerCP-eF710		1:50	Invitrogen	46-0951-82
CD43	FITC		1:300	Biolegend	143203
CD5	APC-eF780	780	1:300	eBioscience	47-0051-80
CD80	BV605		1:200	Biolegend	104729
PDL	SB780		1:300	Invitrogen	78-5982-82
Sca	PerCP-Cy5.5	524	1:500	eBioscience	45-5981-80

Table S3. Solutions used for cell isolation and cell staining protocol

cRPMI
RPMI-1640 with 2mM L-glutamine
10% FCS
1mM sodium pyruvate
1x non-essential AAs
1% penicillin/streptomycin
1:1000 enrofloxacin
1:1000 polymyxin B

Solution 1
1x HBSS
2% FCS
1% penicillin/streptomycin
1:1000 enrofloxacin
1:1000 polymyxin B
1:200 5mM DTT added just before use

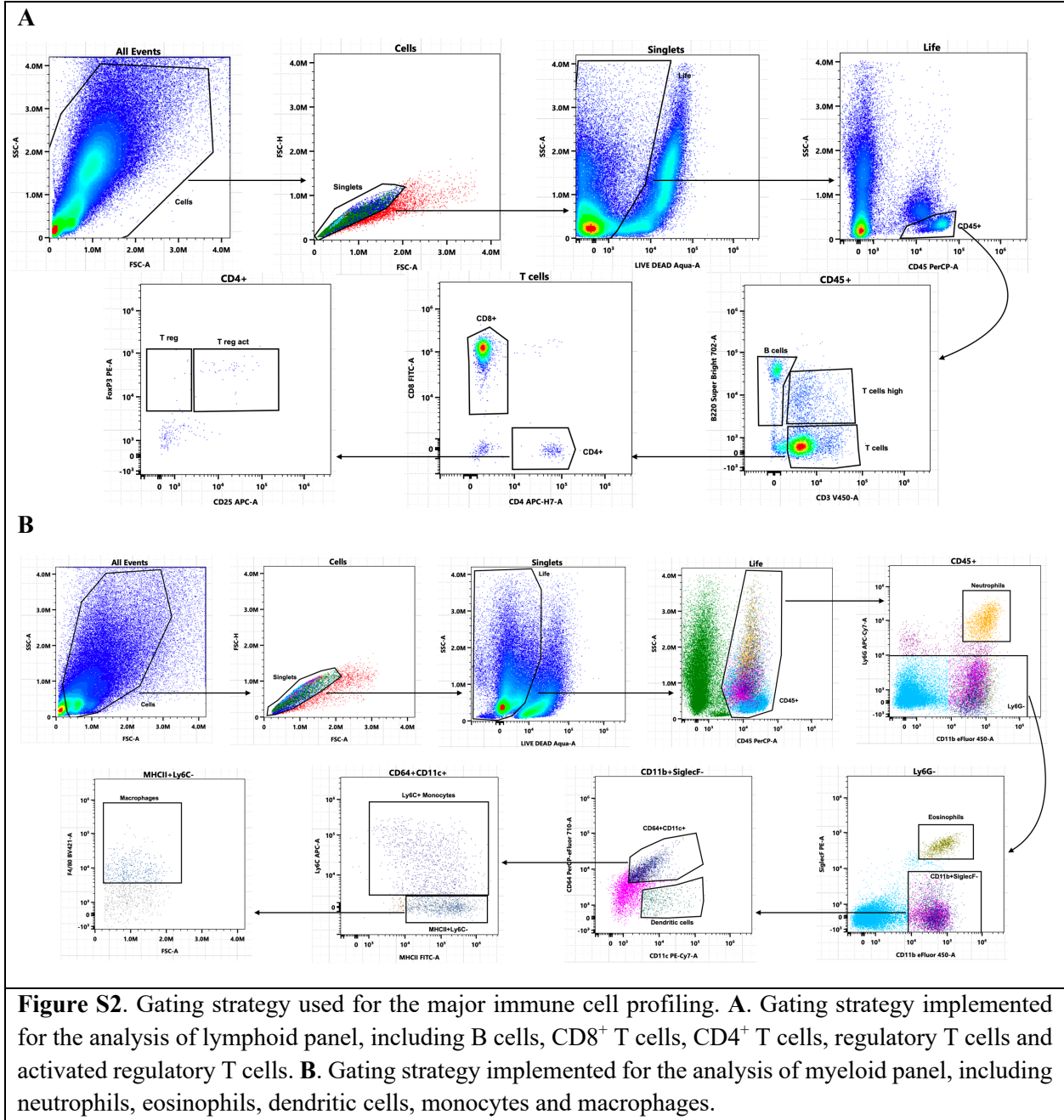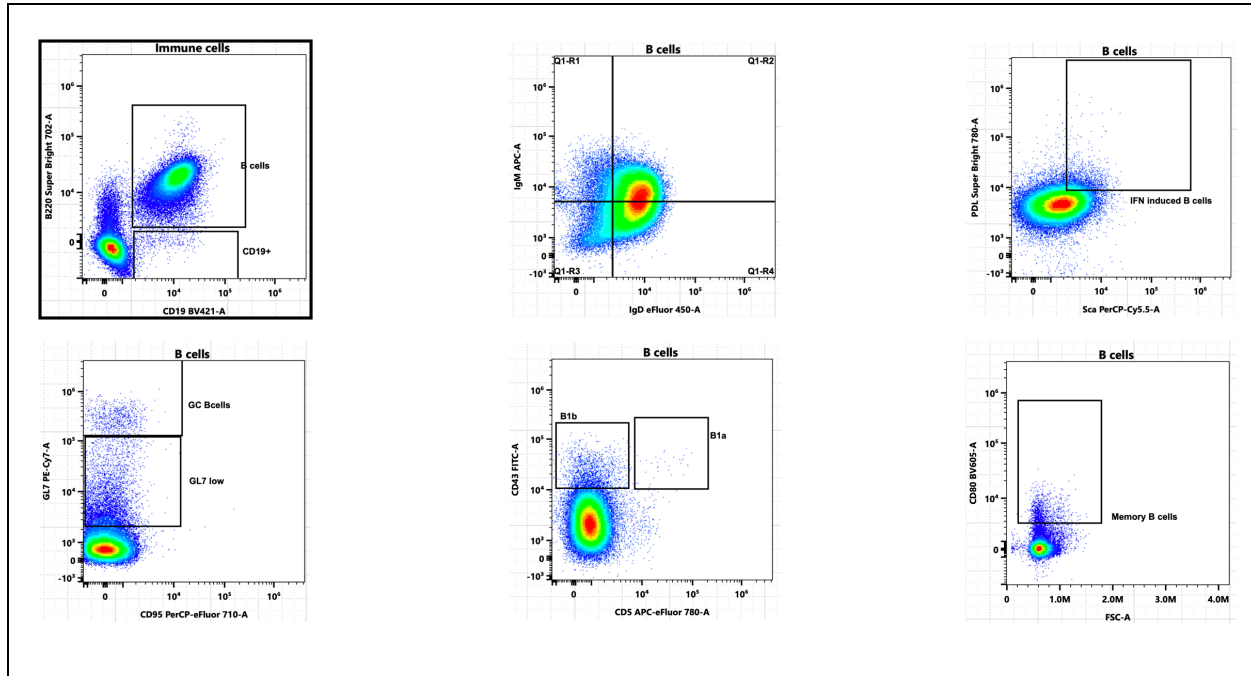| *Solution 2* |
| --- |
| 1x HBSS |
| 2% FCS |
| 1:100 5mM EDTA |
| 1% penicillin/streptomycin |
| 1:1000 enrofloxacin |
| 1:1000 polymyxin B |

| *Solution 3* |
| --- |
| 1x HBSS |
| 1:100 10mM HEPES |
| 1% penicillin/streptomycin |
| 1:1000 enrofloxacin |
| 1:20 20x Liberase stock added just before use |

FACS buffer
Sterile PBS
2% FCS
0.01% sodium azide

Abbreviations - amino acids (AAs); ethylenediaminetetraacetic acid (EDTA); foetal calf serum (FCS); Hank's balanced salt solution (HBSS); phosphate buffer saline (PBS)

Figure S2. Gating strategy used for the major immune cell profiling. **A**. Gating strategy implemented for the analysis of lymphoid panel, including B cells, CD8^{+} T cells, CD4^{+} T cells, regulatory T cells and activated regulatory T cells. **B**. Gating strategy implemented for the analysis of myeloid panel, including neutrophils, eosinophils, dendritic cells, monocytes and macrophages.

Figure S3. Gating strategy used for the analysis of B cell subtypes. The studied B cells are the following: B cells, B1b, B1a, memory B cells, IFN-induced B cells and IgM/IgD B cells. All panels are coming from the same parent panel framed in bold dark. Therefore, the percentage of cells in a specific B cell subtype do not influence the percentage of cells in another B cell subtype.
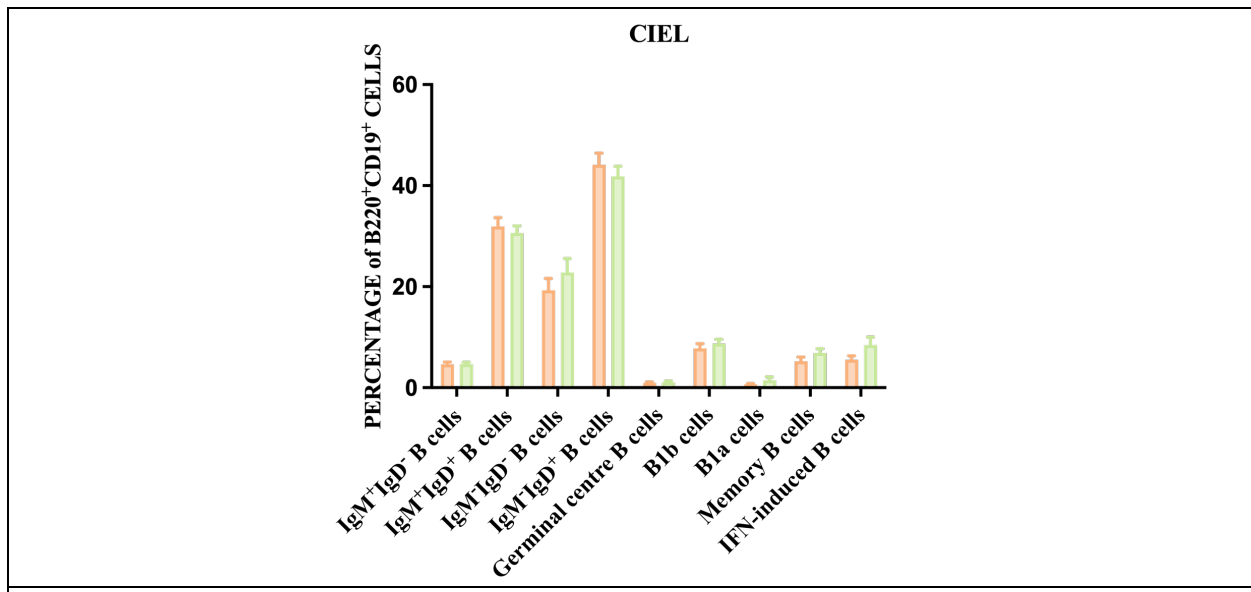
Figure S4. Graphical representation of the results of the B cell subtypes profiling in CIEL samples. No differences in the percentage of different B cell subtypes were observed between Ndrg4$^{fl/fl}$/Wnt1Cre2 (N = 8) and Ndrg4$^{fl/fl}$ mice (N = 8). The analysis included the following B cell subtypes: B1b, B1a, memory B cells, IFN-induced B cells and IgM/IgD B cells. Bars representing mean and SEM calculated with unpaired t-test.
Abbreviation - colonic intraepithelial leukocytes (CIEL)